

Model-based correction of the influence of body position on continuous segmental and hand-to-foot bioimpedance measurements

Guillermo Medrano · Frank Eitner ·
Marian Walter · Steffen Leonhardt

Received: 3 May 2009 / Accepted: 31 March 2010 / Published online: 20 April 2010
© International Federation for Medical and Biological Engineering 2010

Abstract Bioimpedance spectroscopy (BIS) is suitable for continuous monitoring of body water content. The combination of body posture and time is a well-known source of error, which limits the accuracy and therapeutic validity of BIS measurements. This study evaluates a model-based correction as a possible solution. For this purpose, an 11-cylinder model representing body impedance distribution is used. Each cylinder contains a non-linear two-pool model to describe fluid redistribution due to changing body position and its influence on segmental and hand-to-foot (HF) bioimpedance measurements. A model-based correction of segmental (thigh) and HF measurements (Xitron Hydra 4200) in nine healthy human subjects (following a sequence of 7 min supine, 20 min standing, 40 min supine) has been evaluated. The model-based compensation algorithm represents a compromise between accuracy and simplicity, and reduces the influence of changes in body position on the measured extracellular resistance and extracellular fluid by up to 75 and 70%, respectively.

Keywords Segmental · Hand-to-foot · Bioimpedance measurements · Body position · Model-based correction

List of Symbols

α	Heuristic parameter (Cole–Cole model)
c	Circumference
C_{PRO}	Protein concentration
$C_{\text{PRO,P}}$	Protein concentration in plasma
$C_{\text{PRO,IntF}}$	Protein concentration in interstitial fluid
D_{B}	Body density
D_{Muscle}	Density of muscle
IntF_{Rel}	Relative amount of interstitial fluid
K_{f}	Filtration coefficient
$K_{\text{ECF,Muscle}}$	Amount of interstitial fluid per muscle mass
P_{C}	Capillary hydrostatic pressure
Π_{C}	Capillary oncotic pressure
P_{IntF}	Interstitial hydrostatic pressure
Π_{IntF}	Interstitial oncotic pressure
$Q_{\text{L,S}}$	Nominal lymphatic flow for a segment
$Q_{\text{Lymph,S}}$	Effective lymphatic flow for a segment
$Q_{\text{Rel,S}}$	Relative lymphatic flow
$Q_{\text{PI,S}}$	Fluid shift ratio from capillary to interstitial space
ρ_{ECF}	Specific resistivity of extracellular fluid
$R_{\text{V}}/R_{\text{A}}$	Postcapillary to precapillary resistance ratio
R_{e}	Extracellular resistance
R_{i}	Intracellular resistance
T_{D}	Time delay
S	Segment
V_{S}	Segmental volume
V_{B}	Body volume

Abbreviations

BIS	Bioimpedance spectroscopy
ECF	Extracellular fluid
HF	Hand-to-foot
ICF	Intracellular fluid
IntF	Interstitial fluid
PV	Plasma volume

G. Medrano (✉) · M. Walter · S. Leonhardt
Philips Chair for Medical Information Technology (MedIT),
Helmholtz-Institute for Biomedical Engineering, RWTH Aachen
University, Pauwelsstrasse 20, 52074 Aachen, Germany
e-mail: medrano@hia.rwth-aachen.de

F. Eitner
Department of Nephrology (Medical Clinic II), University
Hospital, RWTH Aachen University, Pauwelsstrasse 30,
52074 Aachen, Germany

1 Introduction

Continuous monitoring of body fluids could be a powerful tool for diagnosis in the clinical setting (e.g., for dialysis) or in the home environment (e.g., homes for the elderly). Whereas “dilution methods” are the current gold standard for determination of body water content [29], they are time consuming, expensive, and not suitable for continuous use. In contrast, bioimpedance spectroscopy (BIS) has low costs, allows fast measurements and can be implemented in a portable application [25]. Unfortunately, the negative influence of external factors (e.g., body position and temperature) limits its accuracy. It has been shown that BIS precision can be considerably improved if appropriate physiological modeling is used [6] and the influence of external factors is minimized by establishing standardized “laboratory” conditions [10, 29, 40].

The influence of body position on BIS measurements is based on the redistribution of body fluids [9, 21, 41]. A change from vertical (or sitting) to horizontal position produces a fluid shift from the extremities to the torso [16], causing an increased impedance in the extremities and decreased impedance in the torso [41]. As the torso contributes up to only 5% of the whole body impedance, the measured total body impedance will increase [9, 41]. A change from horizontal to vertical (or sitting) position produces the opposite effect. Interestingly, there is no fast stabilization by remaining in a specific body position (not even after 4 h) [21], and this effect seems to persist throughout the day [37].

To minimize the influence of body position on BIS measurements, recommended “laboratory” conditions include performing measurements in supine position and after a period of recumbance (usually at least 4–10 min) [10, 40], if possible always at the same time of the day [10]. However, in the case of continuous monitoring applications (e.g., during dialysis or intensive care), these laboratory conditions cannot be fulfilled and compensation for the produced error is required. Current methods of correction [9, 41] are neither sufficient to avoid the effect of body position, nor are they suitable for continuous monitoring.

Therefore, the first aim of this study is to evaluate the effectiveness of a model-based compensation for the effects of body position on continuous BIS measurements. The second aim is to develop a model, based on human physiology, able to reproduce the effect of sequential changes in body position on whole body and segmental BIS measurements.

2 Methods

2.1 Bioimpedance spectroscopy

Total body fluid in humans consists of intracellular fluids (ICF) and extracellular fluids (ECF) separated by the

cellular membrane. Due to the predominantly resistive character of ICF and ECF and the capacitive character of the cellular membrane, the path of electrical current through tissue depends on the applied frequency. Low-frequency currents only flow around the cells through the ECF, whereas high-frequency currents will also pass through the cell membrane and ICF. This phenomenon can be represented by the well-known Cole model [35], which represents the tissue using mainly extracellular resistance (R_e) and intracellular resistance (R_i), a capacitor (cell membrane capacitance; C_m) and a heuristic factor (α) representing the presence of different tissues in parallel with specific time constants. Considering this model and a time delay (T_D) produced by the speed of transport of electrical information, the impedance can be expressed as [40]:

$$Z(j\omega) = \left(\frac{R_e}{R_e + R_i} \right) \left(R_i + \frac{R_e}{1 + (j\omega C_m (R_e + R_i))^\alpha} \right) (e^{-j\omega T_D}) \quad (1)$$

Using curve-fitting methods, Eq. 1 and measuring the impedance (Z) at different angular frequencies (ω), the Cole parameters (R_e , R_i , and C_m) can be determined. In fact, typical frequencies lie between 5 kHz and 1 MHz.

Combining these Cole parameters and some basics of Hanai theory [15] and representing body segments as truncated cylindrical volumes, equations for the calculation of whole body and segmental fluid volumes (ECF, ICF, and total body fluid) have been provided in the literature [23, 40]. Accordingly, segmental ECF in (ml) can be calculated as:

$$ECF_S = \frac{\rho_{ECF}^{\frac{2}{3}}}{3 \cdot (4 \cdot \pi)^{\frac{1}{3}}} \cdot l \cdot (c_1^2 + c_1 c_2 + c_2^2) \cdot \left(\frac{l}{c_1 c_2 R_{e,S}} \right)^{\frac{2}{3}}, \quad (2)$$

where l is the segment length (cm), c_1 and c_2 are the segment circumferences (cm) on both ends, and ρ_{ECF} is the specific resistivity of ECF in (Ω cm). For the calculation of whole body fluids (in ml) using the hand-to-foot (HF) measurement, a factor K_B , which relates the relative impact of leg, arm, trunk, and height (H in cm) to the HF measurements, is introduced, and Eq. 2 for HF measurements results in:

$$ECF_{HF} = \left(\frac{K_B^2 \rho_{ECF}^2}{D_B} \right)^{\frac{1}{3}} \left(\frac{H^2 \sqrt{W}}{R_{e,HF}} \right)^{\frac{2}{3}}, \quad (3)$$

where W is the weight (kg) as a measure of body mass and D_B is the body density in (kg/cm^3). Finally, the segmental and whole body ECF can be defined as the addition of interstitial fluid (IntF) and plasma volume (PV) as given by:

$$ECF = IntF + PV \tag{4}$$

2.2 Fluid shifts and body position

A major effect of changing orientation in space is the generation of different hydrostatic blood pressures (Fig. 1) due to gravity.

Changes in blood pressures lead to changes in capillary pressures and, therefore, to fluid shifts between capillary space and surrounding tissue [3]. According to Maw et al. [24], changes in body position do not influence the amount of ICF and fluid shifts take place only within ECF, i.e., between IntF and PV. Therefore, for the present study only changes in ECF (R_e) or in its compartments (IntF and PV) are considered.

2.3 Body posture, bis measurements and model-based correction

The measured R_e value can be represented as a superposition of the influence of time and body posture plus a reference value (e.g., the value measured under the recommended laboratory conditions), see Eq. 5.

$$\underbrace{R_e(\text{measured,time})}_{\text{observed}} = \underbrace{R_e(\text{laboratory conditions})}_{\text{reference}} + \underbrace{\Delta R_e(\text{body posture, time})}_{\text{error}} \tag{5}$$

Assuming that effective changes in body fluid volumes can be measured under laboratory conditions, the observed change in R_e can be expressed rewriting Eq. 5 in terms of an effective body fluid change and the influence of time and body posture:

$$\underbrace{\Delta R_e(\text{measured,time})}_{\text{observed change}} = \underbrace{\Delta R_e(\text{body posture, time})}_{\text{error}} + \underbrace{\Delta R_e(\text{effective change body fluid})}_{\text{effective change}} \tag{6}$$

Thus, for the purpose of this study, the model-based correction yields:

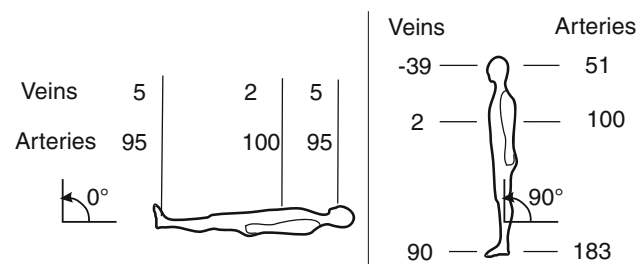


Fig. 1 Typical arterial and venous pressures (mmHg) in supine and vertical position. Assumed body height is 180 cm; values are from [4]

$$\Delta R_e(\text{measured, corrected}) = \Delta R_e(\text{measured,time}) - \Delta R_e(\text{simulation: body posture, time}) \tag{7}$$

The desired result of the simulation is to reproduce the effect of body posture and time ($\Delta R_e(\text{body posture, time}) \cong \Delta R_e(\text{simulation: body posture, time})$) having as a consequence:

$$\Delta R_e(\text{measured, corrected}) \cong \Delta R_e(\text{effective change body fluid}) \tag{8}$$

The error reduction can be quantified using the following equation:

$$\left(1 - \left| \frac{\Delta R_e(\text{measured,time}) - \Delta R_e(\text{simulation body posture,time})}{\Delta R_e(\text{measured,time})} \right| \right) * 100\% \tag{9}$$

2.4 ECF, IntF, and PV in BIS measurements

To evaluate simulations of fluid shifts between IntF and PV, individual measurements of one or of both compartments are required. For that purpose, we propose the approximation of $ECF \cong IntF$ in Eq. 2, i.e., to ignore any electrical conduction through PV, for whole body and segmental limbs measurements. The following facts support this simplification:

- (a) Approximately 75% of muscle tissue is found in the limbs [38]. Assuming that PV is proportional to blood perfusion, 21% of PV is to be found in muscle and therefore only about 16% of the whole PV is found in the limbs.
- (b) Considering a contribution of muscle tissue and PV to body mass of 40 and 4%, respectively [38], PV constitutes only about 2.4% of muscle mass in the limbs and therefore a reduced cross-section compared to muscle tissue.
- (c) Using these facts and assuming that a limb segment can be represented as a circuit with parallel tissues (plasma, muscle, fat, and bone), about 90–95% of the injected current in the limbs will flow through muscle tissue.
- (d) This issue can be extended to HF impedance measurements, since the impedance of the limbs constitutes about 90–95% of the measured HF impedance values [1, 9].

As the amount of PV is very different in the torso this approximation may not be valid for segmental measurements at this location. Note that the result of this analysis is in agreement with reported finite element method simulations [1]. Rewriting Eq. 2, IntF for every segment ($IntF_s$) in ml can be found as:

$$IntF_s = \frac{\rho_{ECF}^{\frac{2}{3}}}{3 \cdot (4 \cdot \pi)^{\frac{1}{3}}} \cdot l \cdot (c_1^2 + c_1 c_2 + c_2^2) \cdot \left(\frac{l}{c_1 c_2 R_{e,S}} \right)^{\frac{2}{3}} \tag{10}$$

2.5 General concept of the model

The proposed model includes two main components:

- An 11-cylinder model representing the body impedance distribution at any time.
- An active nonlinear two-pool model representing fluid shifts between IntF and PV to reproduce changes in impedance with respect to time and body posture in each cylinder (body segment). Fluid shifts outside ECF are not considered.

The general idea of the model for each cylinder is shown in Fig. 2a. Using impedance measured values ($R_{e,S}$) at initial time ($t = 0$) and Eq. 10, initial interstitial fluid segmental volumes (IntF_S) can be calculated. The change in IntF_S with respect to time is calculated with the two-pool model. Now, by knowing the new IntF_S value in time ($t = T$) the new $R_{e,S}$ value is provided as output of Eq. 10. A detailed description of the model is given in the following subsections.

2.6 11-cylinder model

The 11-cylinder model (Fig. 2b) uses the impedance distribution and anthropometric data proposed in [1]. From an electrical point of view, every cylinder represents a body segment and consists of three compartments: IntF, PV, and all other compartments which do not contribute to low frequent current conduction (ICF, bone), see Fig. 2c. HF measurements were simulated as (Fig. 2b):

$$R_{e,HF} = R_{e,calf} + R_{e,knee} + R_{e,thigh} + R_{e,torso} + R_{e,upper\ arm} + R_{e,lower\ arm}, \quad (11)$$

where the subindexes indicate the segmental R_e of the indicated segment (e.g., calf, knee, etc.). The amount of IntF and its distribution (in percentage) were calculated using Eq. 10.

To compare simulations with measurements on subjects, segmental reference dimensions [1] were adapted to the anthropometric characteristics of the subjects as follows:

$$l_{S,adapted} = l_{S,reference} \cdot \frac{H_{subject}}{H_{reference}}, \quad (12)$$

$$c_{S,adapted} = \sqrt{\frac{W_{subject}}{W_{reference}} \cdot \frac{H_{reference}}{H_{subject}}} \cdot c_{S,reference}, \quad (13)$$

where H and W represent the height and weight of the subject, and c and l is the circumference and length of the segments, respectively.

2.6.1 Active nonlinear two-pool model

Fluid shifts between interstitium and plasma in every cylinder are described considering nonlinear effects of protein

concentrations in plasma and the action of the lymphatic pump (Fig. 2d), resulting in the following mass balance (ml/min):

$$\frac{dIntF_S}{dt} = -\frac{dPV_S}{dt} = Q_{PI,S} - Q_{Lymph,S}, \quad (14)$$

where $dIntF_S/dt$, dPV_S/dt represent the change of IntF_S and PV_S with respect to time, $Q_{PI,S}$ and $Q_{Lymph,S}$ are the rate of fluid shift from plasma to interstitium through the capillary membrane and from interstitium to plasma through the lymphatic pump, respectively. $Q_{PI,S}$ in ml/min was calculated using the Starling equation [22]:

$$Q_{PI,S} = K_f \cdot [(P_C - P_{IntF}) - (\Pi_C - \Pi_{IntF})], \quad (15)$$

where capillary hydrostatic pressure (P_C), interstitial fluid pressure (P_{IntF}), plasma oncotic pressure (Π_C), and interstitial fluid oncotic pressure (Π_{IntF}) are expressed in mmHg.

For the filtration coefficient K_f , the value for a human forearm for muscle tissue in [ml/(min*100 g tissue*mmHg)] [22] was used. Muscle tissue was chosen because of its predominance in the limbs, high water content [36] and its decisive role in fluid shifts during body posture manipulations [2]. In case of the lower leg, an additional influence of body posture on the filtration coefficient K_f was considered, according to [7]. The muscle volume (ml) in each cylinder was calculated using the muscle mass (g) and muscle density (D_{Muscle}) in g/ml, according to [38]. The muscle mass was calculated using the amount of IntF at the segment (IntF_S) and the amount of IntF per muscle mass ($K_{ECF,Muscle}$) in ml/g according to [36, 38]. The initial values for P_{IntF} , $C_{Pro,IntF}$, $C_{Pro,P}$ were set according to their normal range found in [13].

P_C was calculated for the middle of the cylinder, using arterial and venous pressure values for supine and vertical positions presented in [4] (Fig. 1) adjusted to anthropometric data, and the ratio of venous to arterial resistance to flow (R_V/R_A), according to [20, 32].

Π_C and Π_{IntF} were calculated as a nonlinear function of the protein concentration (C_{Pro}) as follows [22]:

$$\Pi = 2.1 \cdot C_{Pro} + 0.16 \cdot C_{Pro}^2 + 0.009 \cdot C_{Pro}^3 \quad (16)$$

The change of P_{IntF} was calculated adapting the nonlinear relationship between IntF and P_{IntF} for the whole body to a body segment, adapting the curve presented in [14] in terms of the relative amount of IntF (IntF_{Rel}) to P_{IntF} (Fig. 3, left).

Note that IntF_{Rel} is defined by:

$$IntF_{Rel}(t) = \frac{IntF_S(t)}{IntF_S(0)}, \quad (17)$$

Accordingly, $IntF_{Rel}(0) = 1$ ($P_{IntF} = -3$ mmHg). A mathematical approximation based on the shape of the

Fig. 2 **a** General concept for the model (one segment), **b** 11-cylinder model for the representation of human body with $R_{e,s}$ and IntF distribution ($R_{e,s}$ in (%) of a HF measurement, according to values given by [1]), **c** cylinder model structure, and **d** two-pool model

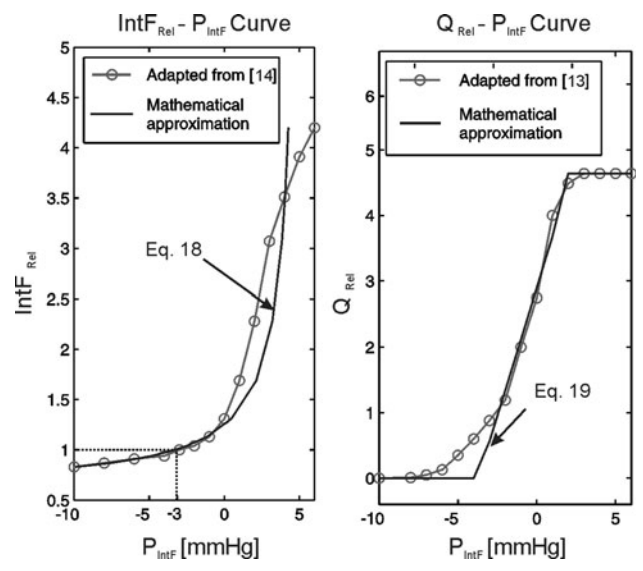
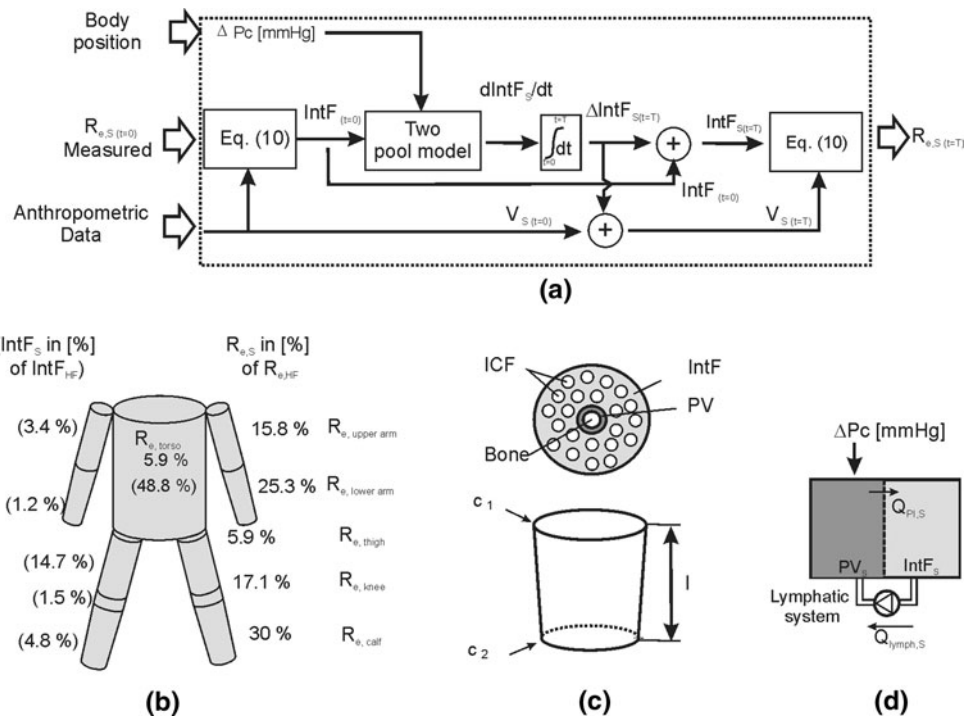


Fig. 3 Relationship between relative IntF, P_{IntF} and relative amount of lymphatic fluid according to [14, 13] and their mathematical approximations: Eqs. 18, 19

function with coefficients calculated using fitting curve algorithms for P_{IntF} in mmHg would be (Fig. 3, left):

$$P_{IntF} = \frac{-1}{0.3(IntF_{Rel} - 0.61)} + 5.17 \quad (18)$$

The lymphatic system was implemented as a mathematical approximation of the curve relating P_{IntF} (mmHg) and the relative lymph flow (Q_{Rel}) as follows (Fig. 3, right):

$$\begin{aligned} Q_{Rel} &= 0 & \forall [P_{IntF}] \leq -3 \\ Q_{Rel} &= 0.78 \cdot P_{IntF} + 2.9 & \forall -3 \leq P_{IntF} \leq 3 \\ Q_{Rel} &= 4.6 & \forall [P_{IntF}] > 3 \end{aligned} \quad (19)$$

Finally, the effective segmental lymph flow, $Q_{Lymph,S}$ (ml/min) is expressed as:

$$Q_{Lymph,S} = Q_{Rel} \cdot Q_{L,S}, \quad (20)$$

where $Q_{L,S}$ is the nominal value for the segment, calculated from the amount of whole body lymph flow (3 l per day [13]), ignoring the lymph flow during 8 h of sleep, and relating it to the segmental (V_S) and the whole body volume (V_B):

$$Q_{L,S} = \frac{3 \text{ l}}{16 \text{ h}} \cdot \frac{1 \text{ h}}{60 \text{ min}} \cdot \frac{V_S}{V_B} \quad (21)$$

In addition a protein concentration for Q_{Lymph} and $Q_{Pl,S}$ of 3 (g/dl) as reported by [16], has been assumed.

Table 1 shows a summary of values used for the model and the respective source. Notice that most of them were taken from the literature (Table 1), with the exception of P_{IntF} for the torso where a value of -1 mmHg was determined from an analysis (for details, see Appendix).

2.7 Study design

Nine healthy volunteers (three females and six males with age, weight, and height averaged \pm SD 26 ± 2.5 years, 66 ± 13 kg and 170 ± 8 cm, and with thigh dimensions c_1 and c_2 of 54.5 ± 5 and 42.7 ± 4.9 cm, respectively) participated in

Table 1 Physiological parameter values used for the initialisation of the model

Parameter	Value	Units	Reference
$C_{Pro,P}$	7.3	g/dl	[13]
$C_{Pro,IntF}$	3.0	g/dl	[13]
D_{Muscle}	1.0414	g/ml	[38]
D_{Body}	1.070	g/ml	[38]
K_f	0.0057	ml/(min*100 g tissue*mmHg)	[22]
$K_{ECF,muscle}$	0.175	ml/g	[36, 38]
PV	3.0	l	[13]
P_{IntF}	-3	mmHg	[13]
P_{IntF} (Torso)	-1	mmHg	Estimated (see Appendix)
R_V/R_A	0.1	-	[20]

this study after giving informed written consent. The study protocol was approved by the local Ethics Committee.

Segmental (thigh) and HF BIS measurements were performed during sequential periods in supine (7 min), vertical (20 min standing), and supine position (40 min) with a commercial bioimpedance device (Xitron Hydra 4200, Xitron Technologies Inc., San Diego, CA, USA) and commercial Al-hydrogel BIS electrodes. Single measurements (repeated 5–6 times every 3–5 s) were performed every 3–4 min. Thigh measurements were followed by HF measurements 1–2 min later.

The measurements were performed in a strictly temperature-controlled room (24°C) always in the morning, 2–3 h after waking up. A period of at least 6 h without eating or drinking and 48 h without strenuous exercise were prerequisites for the tests. Having a fixed distance between the feet, and between arms and torso, the subjects

were advised to remain as still as possible during the measurements. The electrodes were located according to the manufacturer's instructions for the device [40] (Fig. 4), after removing excessive body hair if necessary.

3 Results

Measurements, Simulink® simulations, and model-based corrected measurements for subject 1 (as an example) during the sequence of different body positions for the thigh and HF BIS measurements are shown in Fig. 5a, b, respectively.

The change of R_e with body posture is similar for HF and thigh BIS measurements: they increase during the supine and decrease during the vertical position (Fig. 5). However, changes during standing position are almost twice as fast as changes during the supine position. The measured ΔR_e (in %) for both positions is higher for the thigh than for HF. Similar curves were observed in all subjects, showing differences only in the magnitude of change. The simulations are in agreement with the measurements, allowing an effective reduction of the error produced by body position and time (see Table 2 for details).

For subjects 3 and 5, the 20-min period in a vertical position could not be finished due to symptoms of fainting. The HF and thigh measurements of these two subjects show a higher $|\Delta R_e|$ (in %) during the standing period than in the other subjects (mean \pm SD for the group without these two subjects: -10.86 ± 1.11 for thigh and -3.96 ± 1.32 for HF measurements) and a lower change for the posterior horizontal period (12.49 ± 2.43 and 7.47 ± 0.68 for thigh and HF measurements, respectively). In contrast, subject 4 showed a smaller change during the vertical position HF measurements ($|\Delta R_e|$ in % = -1.4). The ΔR_e (in %; mean \pm SD) for the simulations for the standing period was -13.63 ± 0.20 and

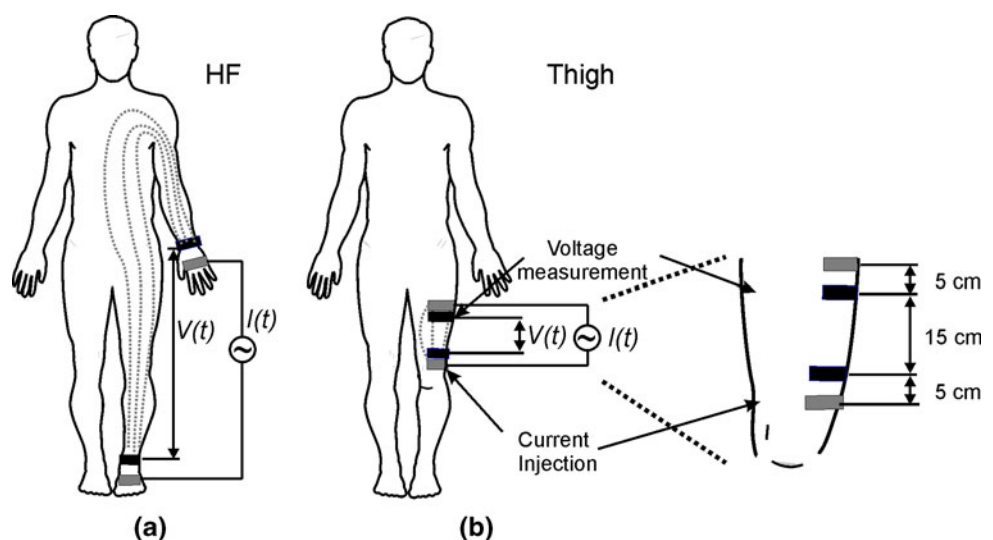
Fig. 4 Diagram showing hand-to-foot and thigh BIS measurements

Fig. 5 Measured, modeled, and corrected R_e trajectories during body position changes for subject 1: **a** for the thigh and **b** for hand-to-foot measurements

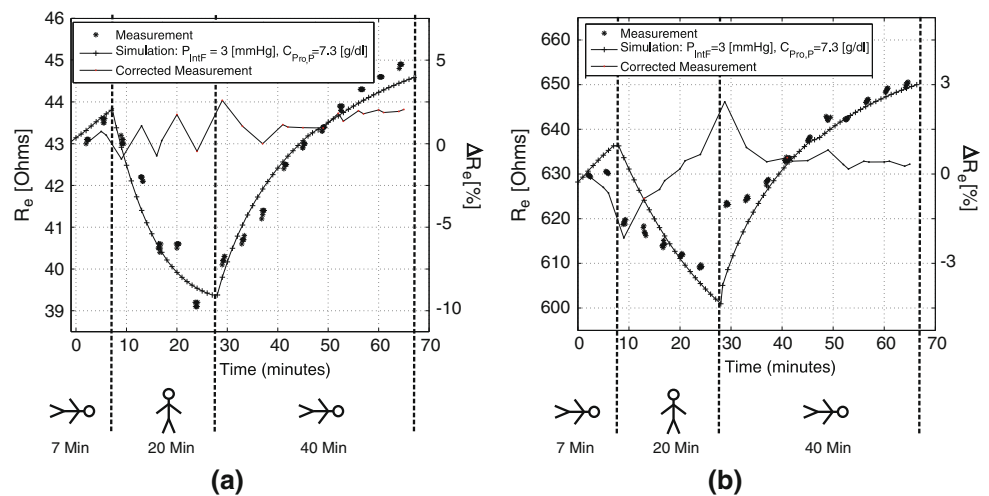


Table 2 Mean \pm SD values of the measured R_e and ECF in all nine subjects (thigh and HF measurements), measured and corrected ΔR_e and ΔECF (in %) of the initial R_e and ECF, and error improvement for the standing (20 min) and supine (40 min) periods

Position (period)	Measured ΔR_e (% R_e)	Corrected ΔR_e (% R_e)	Error reduction in R_e (%)	Measured ΔECF (% ECF)	Corrected ΔECF (% ECF)	Error reduction in ECF (%)
Thigh (initial measured values: R_e (Ω) = 44.02 ± 15.43 , ECF (l) = 0.53 ± 0.15)						
Standing (20 min)	-12.15 ± 2.74	1.48 ± 2.67	75.73 ± 11.17	8.77 ± 2.25	-1.42 ± 2.21	70.20 ± 14.56
Supine (40 min)	12.17 ± 2.80	2.94 ± 2.91	65.36 ± 32.58	-7.70 ± 1.68	2.56 ± 2.10	63.83 ± 24.13
HF (initial measured values: R_e (Ω) = 662.14 ± 89.42 , ECF (l) = 16.14 ± 3.54)						
Standing (20 min)	-4.38 ± 1.47	3.16 ± 1.65	49.43 ± 25.51	2.87 ± 1.06	-2.08 ± 1.09	46.5 ± 27.3
Supine (40 min)	8.03 ± 1.59	1.97 ± 0.67	74.8 ± 13.20	-5.33 ± 1.12	-1.11 ± 1.09	71.6 ± 13.9

-7.29 ± 0.17 for the thigh and HF method, respectively. For the supine period the values were: 15.18 ± 0.22 and 9.45 ± 0.22 (thigh and HF methods, respectively).

For thigh measurements, in both positions the error produced in the measured R_e was about 12%. A model-based correction reduces the error to about 3%, i.e. constituting an error reduction higher than 65% (Table 2: columns 1–3, rows 1 and 2). For the measured ECF, the error was reduced from about 9 to 3%, i.e., an error reduction of more than 60% (see columns 4–6, same rows). For HF measurements, a measured ΔR_e of 8% could be reduced to about 2% (error reduction of about 75%, see columns 1–3, rows 4 and 5). In terms of the measured ECF_{HF} , the error produced during the supine position was about 0.9 l (mean value) which, after the model-based correction, was reduced to about 0.18 l.

4 Discussion

4.1 Model implementation and usability

In the present study, a model based on bioimpedance measurements theory and physiological mechanisms has been

implemented and proposed for reproduction and correction of the effect produced by changes in body position on BIS measurements. The model allows to reproduce the influence of body posture and time on HF and segmental bioimpedance measurements, requiring easy-to-calculate inputs, i.e., anthropometric features of the subjects (or body segment) and data on body posture. The internal calculations are mainly based on published physiological parameters. To our knowledge, only one other study has reproduced the influence of body posture on bioimpedance measurements [26]; however, this latter investigation was dependent on a very approximate reproduction of the change in protein concentration in plasma for the supine position reported elsewhere [16] and, therefore, is not applicable for general use.

The model presented here has been tested only for HF and segmental (thigh) bioimpedance measurements. However, as body posture data are transformed into hydrostatic pressure blood changes, simulations should also be possible for other body positions. In addition, the composition of the model (an 11-cylinder including in each cylinder a two-pool model) allows to simulate changes at almost any body segment, based on fluid shifts between capillary space and interstitial fluid. As several processes that affect impedance measurements are related to body fluid redistribution between those spaces (e.g.,

ambient temperature, food and fluids consumption, ultrafiltration, changes in body posture) [5, 21, 27, 34], in the future the present model might be used to investigate or reproduce some of these processes. The correction of segmental bioimpedance measurements on specific body postures may be of future importance [17, 27, 34].

Despite these advantages, the model requires a relatively large amount of variables, which could limit its use to clinical research only. Future investigations should focus on simplification of the model for specific applications.

4.2 Model-based correction as an alternative

Based on our results from nine healthy subjects, the model-based correction allows an error reduction of the influence of body position (vertical and horizontal) of 65–75% and of 45–72% for segmental (thigh) and whole body (HF) R_e measurements. A smaller error reduction was obtained for the standing position (HF measurements).

The two methods currently proposed to reduce the influence of body posture and time are: (1) parallel measurement of torso and extremities, which showed an error reduction of about 100% for ECF (HF) measurements according to [41] (11 subjects), and of only 25% according to [9] (15 subjects) and (2) starting measurements about 20 min after lying supine which, according to our measurements, may reduce the error by 50–60% for a 40-min period of recumbancy; however, for longer periods the effectivity decreases with increasing length of the measurement period (e.g., only about 30% for a 4-h supine period). In clinical use (e.g., during dialysis), body fluid changes (e.g., ultrafiltration) and fluid redistribution produced by continuous changes of body posture and time may take place at the same time. This combined effect is only taken into account by method 1 and by model-based correction. From the present, study the following conclusions can be drawn: in terms of effectivity, the model-based correction can be better than method 2, but may not be as effective as method 1. In terms of comfort, model-based correction is as good as method 2.

Even though model-based correction allows a reduction of the magnitude of the error, further improvements are possible. During the evaluation periods, differences between simulations and measurements sometimes produced a corrected signal with undesired peaks and an overcorrection of the error (Fig. 5, Table 2). Possible reasons for these differences are measurement conditions, and limitations of the model.

4.2.1 Measurement conditions

As changes between HF and thigh measurements were performed manually, some error between measurements could be

produced by handling. In addition, in some cases involuntary muscle movements were observed in the subjects during the measurements (mainly during standing), which could lead to differences between simulations and measurements.

4.2.2 Limitations of the model

Even though the model takes important physiological mechanisms into consideration, some limitations can be identified. These are discussed below.

4.2.3 Validity of the model for all segments

As discussed in the Sect. 2.4, Eq. 10 is valid for the limbs due to the high amount of muscle compared to blood (PV). However, changes in body posture can expand the PV compartment, thus changing the amount of conduction through blood. From our calculations these changes at the thicker part of the calf can produce a change of current conduction through blood only from 2.5 (supine) to 6.4% (standing). However, the lower part of the calf presents much less muscle tissue and a large contribution to the measured HF impedance. Changes in PV at this part may have a greater influence than changes in PV at other limb segments; this indicates that immediate changes in HF impedance after changes in body posture mainly reflect changes in intravascular volume, while posterior changes are mainly due to capillary filtration, as suggested by [11]. This would explain the fast changes in impedance after changing body posture seen in the HF measurements, but not in the thigh measurements (Fig. 5).

4.2.4 Consideration of individual differences

The model takes anthropometric differences between subjects into consideration; however, a relatively low SD for the simulations did not follow the moderately high SD of the measurements. As relatively high SD values in measurements have been reported by others [9, 41], the low SD of the simulations indicates differences between subjects not yet taken into consideration in the model. To establish which model variables play a major role in the tuning with measurements, a sensitivity analysis was performed. The results indicate that all factors with a large influence on ΔR_e (%) are of a physiological character (e.g., $C_{Pro,P}$ and $IntF$ (P_{IntF})), while anthropometric factors (e.g., external dimensions of the thigh and differences in segments length) seem to play an important role only in the calculation of the initial R_e . As the model requires a measured R_e as initial value, small inaccuracies in anthropometric data (e.g., the use of Eqs. 12, 13) will have a reduced effect on the results. The two physiological factors with the greatest effect on the results were the concentration of proteins in

plasma ($C_{Pro,P}$), and the amount of IntF (P_{IntF}). Their influence on the fluid shift rate between interstitium and capillary spaces has been reported in simulations [5] and measurements [11] and is interrelated with fluid volume state (see Fig. 3). As the normal range for these values [12, 38, 39] is high enough to influence the simulation results, their influence is highly likely (see Appendix for details). $C_{Pro,P}$ and P_{IntF} are prime candidates for the tuning of simulations and measurements in future investigations. Other physiological parameters related with microcirculation (e.g., K_f , R_A/R_V), which could be different between individuals [28] showed less influence in the simulations.

Note that in the present study, the influence of fluid shifts between ECF and ICF has been ignored and the model corrects only R_e values. Although changes in R_i due to body posture and time have been reported, these changes appear to be much smaller than R_e changes [9], which supports the findings of Maw et al. [24] and the assumption for the present research. Based on this assumption, the influence of body posture on BIS measurements is due to ECF redistributions between the torso (containing almost 50% of body water) and the limbs representing almost 90% of the measured HF impedance [1, 9, 41]. Small changes in fluid volume in the limbs are “more visible” than changes in the torso. Model-based simulations could be the key to predict these “invisible” changes in body fluid and thereby avoid errors due to fluid redistributions. Even so the present model needs R_e values as input, impedance values at specific frequencies could be used [18, 19, 33].

In conclusion, we argue that the influence of body posture and time is unavoidable on every bioimpedance measurement. However, the proposed model and model-based correction procedure constitute a new and effective alternative to reduce the influence of body posture on segmental and HF bioimpedance measurements. Since the model is based on human anatomy and physiology and only requires as input data easy to obtain, its application is very suitable in clinical research. Further investigation may improve the model accuracy and extend its application for the correction of other influences affecting the accuracy of bioimpedance measurements.

Acknowledgments Special thanks go to Dr. Chamney, Dr. Wabel, and Dr. Moissl at Fresenius Medical Care GmbH for their help with the literature and for interesting discussions. This work was partially supported by the Science and Technology National Board of the Mexican government (CONACYT).

Appendix

Calculation of P_{IntF} for the torso

Fluid shifts from the legs to the torso for the change of vertical to supine position, and vice versa, as observed

through bioimpedance [9, 35, 41] and computer tomography [2] measurements. Accordingly, fluid in the torso should flow from the capillaries into the interstitium during supine position and in the opposite direction during standing position. Values reported for the chest (lungs capillaries) [13] were taken to capture the effect of Starling’s forces in the torso, resulting in the right direction during supine (Fig. 6a, left), but in the opposite direction during standing position (Fig. 6a, right).

To satisfy the desired result during standing position, the following relation must be fulfilled:

$$P_C + P_{IntF} + \Pi_{IntF} < \Pi_C \tag{22}$$

Equation 22 indicates that during a change from supine to standing position, a fast change in one of the pressures (in addition to the change already considered in P_C) is necessary. As a fast change in Π_{IntF} and Π_C is not expected [16, 30] the values for P_C , Π_{IntF} , and Π_C for the standing position can be substituted on Eq. 22:

$$12 + P_{IntF} + 14 < 28 \text{ (mmHg)} \tag{23}$$

$$P_{IntF} < 2 \text{ (mmHg)} \tag{24}$$

Considering the directions of the arrows, a value of $|P_{IntF}| = 1 \text{ mmHg}$ (physiologically -1 mmHg) during standing position was assumed. The result can be seen in Fig. 6b. Explanations for this value could be: (a) the influence of gravity in the pleura (standing position should lead to a reduction of $|P_{IntF}|$ [31] or (b) an increase in the intraperitoneal pressure in the lower part of the abdomen [8], producing a reduction of $|P_{IntF}|$.

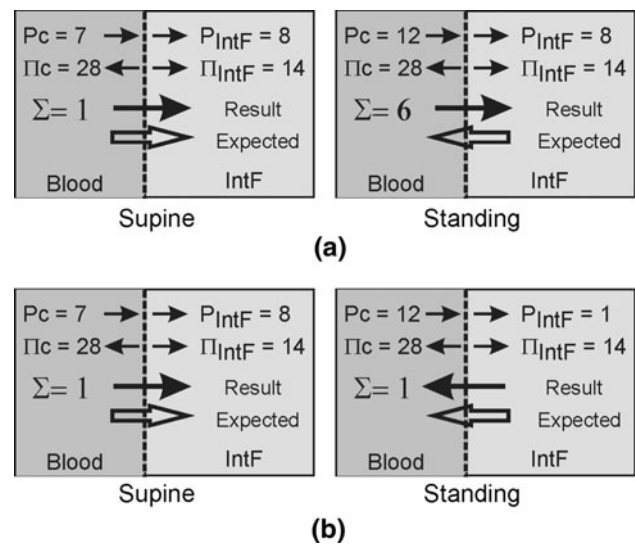


Fig. 6 Starling’s forces in the torso (in mmHg, signs have been represented as directions) and expected and produced direction of the fluid shift between interstitial and capillary spaces for supine and standing position. **a** Π_C , Π_{IntF} , and P_{IntF} according to [13]. P_C as explained in the Sect. 2.6.1. **b** P_{IntF} according to analysis (see text)

Table 3 Influence of using initialisation values +10% on the simulated ΔR_e (%) and R_e (%)

Parameter	Thigh			Hand-to-foot		
	Initial R_e (%)	ΔR_e (%) standing position 20 min	ΔR_e (%) supine position 40 min	Initial R_e (%)	ΔR_e (%) standing position 20 min	ΔR_e (%) supine position 40 min
↑ $C_{Pro,p}$	0.0	↓ 1.37	↑ 2.86	0.0	↓ 1.49	↑ 2.17
↑ IntF (P_{IntF})	0.0	↓ 1.33	↑ 3.37	0.0	↓ 0.43	↓ 2.55
↑ R_v/R_A	0.0	↑ 0.24	↓ 0.46	0.0	↑ 0.13	↓ 0.29
↑ K_f	0.0	↑ 0.20	↓ 0.33	0.0	↑ 0.44	↓ 0.92
↑ Anthropometric (asymmetric)	↑ 2.26	↓ 0.10	↑ 0.15	↑ 2.51	↓ 0.05	↑ 0.08
↑ Anthropometric (symmetric)	↑ 0.43	↓ 0.02	↑ 0.02	↑ 0.43	↓ 0.01	↑ 0.01

(↑) represents an increase and (↓) a decrease

Sensitivity analysis

The influence of model parameter values on ΔR_e has been determined through simulations using nominal parameter values +10%. Anthropometric changes influenced only the initial R_e value. Changes in the amount of proteins ($C_{Pro,p}$) and in fluid volume state (IntF (P_{IntF})) present a relatively large influence on the simulated ΔR_e (see details in Table 3).

Suitability of the influence of different $C_{Pro,p}$ and IntF (P_{IntF}) values on ΔR_e :

- As healthy $C_{Pro,p}$ can range from 6.5 to 7.2 g/dl (reference [38]) or even between 6.4 and 8.3 g/dl (reference [12]), which is more than +10%, this parameter may influence the differences between simulations and measurements.
- Since a mild dehydration constitutes a loss of 3% of body weight and about 20% of ECF without presenting any clear symptoms [39], a local change of IntF by 10% is very possible and the local P_{IntF} for each subject could vary from the assumed initial $P_{IntF} = -3$ mmHg.

References

- Barchansky A (2007) Simulations of low-frequency electromagnetic fields in the human body. PhD thesis. Technical University Darmstadt, Germany
- Berg H, Tedner B, Tesch P (1993) Changes in lower limb muscle cross-sectional area and tissue fluid volume after transition from standing to supine. *Acta Physiol Scand* 148:379–385
- Blomqvist C, Lowell H (1983) Cardiovascular adjustments to gravitational stress. In: Handbook of physiology, The cardiovascular system. Peripheral circulation and organ blood flow, sect 2, vol III, pt 2, chap 28. Am. Physiol. Soc., Bethesda, pp 1025–1063
- Burton A (1969) Physiologie und Biophysik des Kreislaufs. 1969. From the original Physiology and biophysics of the circulation 1965. F.K. Schattauer Verlag, Stuttgart
- Chamney P, Johner C, Aldridge C, Kramer M, Valasco N, Tattersall J, Aukaidey T, Gordon R, Greenwood R (1999) Fluid balance modelling in patients with kidney failure. *J Med Eng Technol* 23(2):45–52
- Chamney P, Wabel P, Moissl U, Müller M, Bosy-Westphal A, Korth O, Fuller N (2007) A whole-body model to distinguish excess fluid from the hydration of major body tissues. *Am J Clin Nutr* 85:80–89
- Christ F, Gamble J, Baranov V, Kotov A, Garside I, Nehring I, Messmer K (1999) Microvascular fluid filtration capacity (k_f) assessed with cumulative small venous pressure steps and various degrees of tilt. *Eur J Med Res* 4:264–270
- Drye J (1948) Intraperitoneal pressure in the human. *Surg Gynecol Obstet* 87:472–475
- Fenech M, Jaffrin M (2004) Extracellular and intracellular volume variations during postural change measured by segmental and wrist-ankle bioimpedance spectroscopy. *IEEE Trans Biomed Eng* 51(1):166–175
- Fresenius Medical Care (2006) Body composition monitor (BCM). Operating instructions. Fresenius Medical Care
- Gamble J, Gartside I, Christ F (1993) A reassessment of Mercury in silastic strain gauge plethysmography for the microvascular permeability in man. *J Physiol* 464:407–422
- Guder W, Nolte J (2005) Das Laborbuch für Klinik und Praxis, 1st edn. Elsevier, München
- Guyton A, Hall J (2006) Textbook of medical physiology, 11th edn. Elsevier/Saunders, USA
- Guyton A, Granger H, Taylor A (1971) Interstitial pressure. *Physiol Rev* 51(3):527–563
- Hanai T (1968) Electrical properties of emulsions. In: Sherman P (ed) Emulsions science. Academic Press, London, pp 374–475
- Hinghofer-Szalkay H, Moser M (1986) Fluid and protein shifts after postural changes in humans. *Am J Physiol* 250:H68–H75
- Hong KH, Lim YG, Park KS (2009) Effectiveness of thigh-to-thigh current path for the measurement of abdominal fat in bioelectrical impedance analysis. *Med Biol Eng Comput* 47:1265–1271
- Jaffrin M, Morel H (2009) Extracellular volume measurements using bioimpedance spectroscopy-Hanai method and wrist-to-ankle resistance at 50 kHz. *Med Bio Eng Comput* 47:77–84
- Jaffrin M, Fenech M, Moreno MV, Kieffer R (2006) Total body water measurement by a modification of the bioimpedance spectroscopy method. *Med Bio Eng Comput* 44:873–882
- Klabunde R (2005) Cardiovascular physiology concepts. Ed. Lippincott Williams & Wilkins, USA
- Kushner R, Gudivaka R, Schoeller D (1996) Clinical characteristics influencing bioelectrical impedance analysis measurements. *Am J Clin Nutr* 64(3 Suppl):423–427
- Landis E, Pappenheimer J (1963) Exchange of substances through the capillary walls. In: Hamilton W, Dow P (eds) Handbook of physiology. Waverly Press, Washington DC, pp 961–1034

23. Matthie J (2005) Second generation mixture theory equation for estimating intracellular water using bioimpedance spectroscopy. *J Appl Physiol* 99:780–781
24. Maw G, Mackenzie I, Taylor N (1995) Redistribution of body fluids during postural manipulations. *Acta Physiol Scand* 155: 157–163
25. Medrano G, Beckmann L, Zimmermann N, Grundmann T, Gries T, Leonhardt S (2007) Bioimpedance spectroscopy with textile electrodes for a continuous monitoring application. In: Fourth international workshop on wearable and implantable body sensor networks (BSN), Aachen, IFMBE proceedings, vol 13, pp 23–28
26. Medrano G, Leonhardt S, Zhang P (2007) Modeling the influence of body position in bioimpedance measurements. In: Proceedings of the 29th annual international conference of the IEEE EMBS. Cité Internationale, Lyon, France, pp 3934–3937
27. Medrano G, Eitner F, Floege J, Leonhardt S (2010) A novel bioimpedance technique to monitor fluid volume state during hemodialysis treatment. *ASAIO J* 56(3) (in press)
28. Mitchell G (2009) Clinical achievements of impedance analysis. *Med Biol Eng Comput* 47:153–163
29. Moissl U, Wabel P, Chamney P, Bosaeus I, Levin N, Bosy-Westphal A, Korth O, Müller M, Ellegård L, Malmros V, Kait-watcharachai Ch, Kuhlmann M, Zhu F, Fuller N (2006) Body fluid volume determination via body composition spectroscopy in health and disease. *Physiol Meas* 27:921–933
30. Noddeland H (1982) Influence of body posture on transcapillary pressures in human subcutaneous tissue. *Scand J Clin Lab Invest* 42:131–138
31. Oczenski W, Werba A, Andel H (1997) Breathing and mechanical support, 3rd edn. Blackwell Science, Berlin
32. Pappenheimer J, Soto-Rivera A (1948) Effective osmotic pressure of the plasma proteins and other quantities associated with capillary circulation in the hindlimbs of cats and dogs. *Am J Physiol* 152:471–491
33. Paterno A, Stiz R, Bertemes-Filho P (2009) Frequency-domain reconstruction of signals in electrical bioimpedance spectroscopy. *Med Biol Eng Comput* 47:1093–1102
34. Sakamoto K, Kanai H, Furuya N (2004) Electrical admittance method for estimating fluid removal during artificial dialysis. *Med Biol Eng Comput* 42:356–365
35. Scharfetter H, Monif M, László Z, Lambauer T, Hutten H, Hinghofer-Szalkay H (1997) Effect of postural changes on the reliability of volume estimations from bioimpedance spectroscopy data. *Kidney Int* 51:1078–1087
36. Skelton H (1927) The storage of water by various tissues of the body. *Arch Int Med* 40:140
37. Slinde F, Bark A, Jansson J, Rossander-Hulthén L (2003) Bioelectrical impedance variation in healthy subjects during 12 h in the supine position. *Clin Nutr* 22(2):153–157
38. Snyder W, Cook M, Nasset E, Karhausen L, Howells P, Tipton I (1975) Report of the task group on reference man, international commission on radiological protection (ICRP), report no. 23. Pergamon Press, Oxford
39. Winter R (1973) The body fluids in pediatrics. Medical, surgical and neonatal disorders of acid-basis status, hydration and oxygenation. Little, Brown and Company, Boston
40. Xitron Technologies (2001) Hydra ECF/ICF (Model 4200), Bioimpedance spectrum analyser. Operating manual, Xitron Technologies Inc., San Diego
41. Zhu F, Schneditz D, Wang E, Levin NW (1998) Dynamics of segmental extracellular volumes during changes in body position by bioimpedance analysis. *J Appl Physiol* 85:497–504